Phosphoisoprenoid Binding Specificity of Geranylgeranyltransferase Type II

Nicolas H. Thomä, Andrei Iakovenko, David Owen,‡ Axel S. Scheidig, Herbert Waldmann, Roger S. Goody, and Kirill Alexandrov*

Max-Plank-Institute for molecular Physiology, Otto-Hahn-Strasse 11, 44227 Dortmund, Germany

Received April 12, 2000; Revised Manuscript Received July 5, 2000

ABSTRACT: Geranylgeranyltransferase type II (GGTase-II) modifies small monomeric GTPases of the Rab family by attaching geranylgeranyl moieties onto two cysteines of their C-terminus. We investigated to what extent GGTase-II discriminates between its native substrate geranylgeranyl pyrophosphate (GGpp) and other phosphoisoprenoids, including farnesyl pyrophosphate (Fpp). On the basis of a novel fluorescent assay, we demonstrated that GGpp binds to GGTase-II with an affinity of 8 ± 4 nM, while Fpp is bound less strongly ($K_d = 60 \pm 8$ nM). Analysis of the binding kinetics of four different phosphoisoprenoids indicated that in all cases association is rapid, with rate constants in the range of 0.15 nM^{-1} s^{-1}. In contrast, the dissociation rates differed greatly, depending on the phosphoisoprenoid used, with weak binding substrates generally displaying an increased rate of dissociation. The affinity of GGpp and Fpp for GGTase-II was also determined in the presence of the Rab7−REP-1 complex. The affinity for GGpp was essentially unaffected by the presence of the complex; Fpp on the other hand bound less strongly to the GGTase-II under these conditions, resulting in a K_d of 260 ± 60 nM. In vitro prenylation experiments were used to establish that Fpp not only does bind to GGTase-II but also is transferred with an observed rate constant of 0.082 s^{-1} which is very similar to that of GGpp. The implications of the low level of discrimination by GGTase-II for the in vivo specificity of the enzyme and the use of farnesyltransferase inhibitors in anti-cancer therapy are discussed.

Over the past several years, it has become increasingly clear that posttranslational modification with isoprenoids is a widespread phenomenon, affecting up to 2% of proteins in eukaryotic cells (*1*, *2*). In all the cases that have been studied, such modification was found to be crucial for the protein function (modulating protein−protein or protein−lipid interaction). Many prenylated proteins, predominantly GTPases, play key roles in signal transduction pathways. This includes subunits of heterotrimeric G proteins and many proteins of the Ras superfamily. Interest in protein prenylation increased dramatically following the recognition of the importance of this modification for sustaining the transformed phenotype in many cell lines (*3*, *4*).

In protein prenylation, either a farnesyl or a geranylgeranyl moiety is donated by soluble phosphoisoprenoids and attached to one or two C-terminal cysteine residues of the target protein via a thioether linkage. This type of reaction is catalyzed by three different protein prenyl transferases: protein farnesyltransferase (FTase),[1] protein geranylgeranyl transferase I (GGTase-I), and Rab geranylgeranyl transferase (GGTase-II) (for a review, see ref *5*). The closely related FTase and GGTase-I transfer prenyl groups from prenyl pyrophosphates to proteins that contain a C-terminal CAAX motif (C is cysteine, A is usually an aliphatic amino acid, and X is a variety of amino acids). The X residue of this motif largely determines the choice of isoprenoid.

GGTase-II stands quite apart from the above-mentioned enzymes both functionally and structurally. Mammalian GGTase-II is a heterodimer composed of α and *β* subunits of 60 and 38 kDa, respectively, and the structure of the enzyme has recently been determined at 2 Å resolution (*6*). GGTase-II possesses only one prenyl binding site, which appears deeper then was previously observed in farnesyltransferase (*7*). The enzyme transfers the geranylgeranyl moiety onto two C-terminal cysteines of Rab proteins in a broad context of amino acids (*5*). In contrast to other known prenyl transferases, GGTase-II does not recognize its substrate directly, but exerts its function in concert with another protein termed REP (Rab escort protein) (*8*, *9*). According to the current model, a newly synthesized Rab protein forms a stable complex with REP. GGTase-II recognizes the Rab−REP complex and covalently attaches the geranylgeranyl groups to two C-terminal cysteines of the Rab protein (*5*). Upon prenylation, the Rab−REP complex is believed to dissociate from GGTase-II and escort Rab to its target membrane (*10*, *11*).

At present, there are no direct data available concerning the affinity of GGTase-II for isoprenoids or about the kinetic mechanism of the binding reaction. On the basis of previous competition experiments, however, it has been proposed that Fpp is not a substrate of GGTase-II (*12*). This information

* To whom correspondence should be addressed. Telephone: +49 231 1332356. Fax: +49 231 1331651. E-mail: kirill.alexandrov@mpi-dortmund.mpg.de.

‡ Present address: Department of Medicinal Chemistry, Victorian College of Pharmacy, Monash Univeristy, 381 Royal Parade, Parkville Melbourne, Victoria 3052, Australia.

[1] Abbreviations: Fpp, farnesyl pyrophosphate; FRET, fluorescence resonance energy transfer; FTase, protein farnesyltransferase; GGTase-I, protein geranylgeranyltransferase type I; GGTase-II, geranylgeranyltransferase type II; GGpp, geranylgeranyl pyrophosphate; mant, *N*-methylanthraniloyl; mFpp, mant-labeled farnesyl pyrophosphate; mGpp, mant-labeled geranyl pyrophosphate; Rab7-SS, Rab7 C205S and C207S double mutant.

10.1021/bi000835m CCC: $19.00
Published on Web 09/02/2000

is also clinically relevant due to the increasing number of prenyl transferase inhibitors intended for cancer and kinetoplastid parasite therapy, where inhibition of GGTase-II constitutes an undesired side effect (*3*, *4*, *13*).

In this study, we demonstrate that Fpp is a substrate for GGTase-II and that it is incorporated into Rab7 at a rate equal to that for GGpp. We also show that GGpp binds to GGTase-II with an affinity of around 10 nM, while Fpp is bound between 7- and 20-fold less strongly by GGTase-II and the GGTase-II−Rab7−REP-1 complexes, respectively. These data demonstrate that GGTase-II is less specific toward its lipid substrate than previously believed.

MATERIALS AND METHODS

Preparation of Fluorescent Analogues of GGpp and Fpp. Synthesis of the fluorescently labeled analogues of GGpp and Fpp was performed as described previously (*14*). Fluorescent phosphoisoprenoids were stored as 20 mM solutions in 25 mM $(NH_4)_2CO_3$ at −80 °C.

Expression and purification of mammalian GGTase-II were performed as described in ref *15*.

Purification of the Rab7−REP-1 and Rab7C205S/C207C−REP-1−GGTase-II Complex. Protein complex formation was performed in 1 mL of 40 mM Hepes (pH 7.2), 150 mM NaCl, 5 mM DTE, and 3 mM $MgCl_2$ for 5 min on ice. Depending on the experiment, the 1 mL mixture contained 50 μM REP-1, 100 μM Rab7, and, in the case of the ternary complex, 80 μM GGTase-II. The sample was mixed, centrifuged in a benchtop centrifuge for 5 min, and loaded onto a 16/60 Superdex 200 gel filtration column (Pharmacia). The flow rate was 2 mL/min. The resulting fractions were analyzed by SDS−PAGE followed by Coomassie Blue staining. Fractions containing the binary or ternary complex were pooled, concentrated, and stored in multiple aliquots at −80 °C.

In Vitro Prenylation Assay. The in vitro prenylation reactions were performed essentially as described in ref *16*. Briefly, in a typical reaction volume of 50 μL, 10 pmol of the purified REP-1−Rab7 complex was mixed with 30 pmol of GGTase-II. The reaction was initiated by the addition of 100 pmol of geranylgeranylpyrophosphate or farnesylpyrophosphate with a specific radioactivity in the range of 5000 cpm/pmol. All reactions were carried out at 30 °C in 25 mM Hepes (pH 7.2), 40 mM NaCl, 2 mM $MgCl_2$, 2 mM DTE, and 1 mM NP40. After defined time intervals, the reaction was quenched by addition of 2 mL of 10% HCl in 90% ethanol (v/v). The solution was incubated for 30 min at room temperature and was subsequently filtered through glass fiber filters (Whatman). The filters were washed twice with 96% ethanol, immersed in scintillation liquid, and counted for ^3H.

Fluorescent Measurements. Fluorescence spectra and long-time base fluorescence measurements were performed with an Aminco SLM 8100 spectrophotometer (Aminco). Reactions were carried out at 25 °C in 25 mM Hepes (pH 7.2), 40 mM NaCl, 2 mM $MgCl_2$, 2 mM DTE, and 100 μM GDP. Stopped-flow experiments were performed in an SF61 apparatus (High-Tech Scientific).

Analysis of Titrations of Mant-Labeled Phosphoisoprenoid versus Increasing Concentrations of GGTase-II. Titrations were fitted to the explicit solution of the quadratic equation describing the $E + S \rightleftarrows ES$ binding equilibrium, where K_d is defined as $K_d = [E][S]/[ES]$. For titrations performed in this study, the concentration of the mant-labeled phosphoisoprenoid was fixed ($[S_0]$), and increasing concentrations of GGTase-II ($[E_0]$) were added. $[E_0]$ and $[S_0]$ refer to the total concentration, free and bound, of the enzyme and substrate in the cuvette, respectively. Under these conditions, the fluorescence is described by

$$F = F_{min} + [(F_{max} - F_{min})/[S_0]]([E_0] + [S_0] + K_d)/2 - [([E_0] + [S_0] + K_d)^2/4 - [E_0][S_0]]^{1/2}$$

where F represents the measured fluorescence intensity and F_{min} and F_{max} refer to the minimal and maximal observed fluorescence intensity, respectively. It should be noted that the quadratic equation is generally valid, but simplifies to a simple hyperbolic relationship if $[E_0] \gg [S_0]$, since the hyperbolic equation relates the degree of saturation to the free substrate concentration.

Analysis of Competitive Titrations. Competitive titrations were performed by titrating a mixture of mant-labeled and unlabeled phosphoisoprenoid against increasing concentrations of GGTase-II. The GGTase-II added under these conditions will partition between the fluorescently labeled and the unlabeled phosphoisoprenoid. If, at prevailing concentrations, the unlabeled substrate binds more tightly to GGTase-II than the fluorescently labeled substrate, then the observed titration curve will appear to be sigmoidal. This behavior is due to GGTase-II binding preferentially to the unlabeled substrate and therefore not giving rise to an increase in fluorescence. However, as the concentration of GGTase-II is increased, binding of the unlabeled substrate will saturate, and more of the enzyme will bind to the mant-labeled substrate, giving rise to an increase in fluorescence. The exact shape of the curve depends not only on the relative K_ds but also on their magnitude. This is in contrast to the situation in which fluorescent ligand is displaced form its preformed complex with protein by the unlabeled ligand, which in general only gives information about the relative K_ds. However, since the exact affinity of the fluorescently labeled phosphoisoprenoid toward GGTase-II is known from direct experiments (see above), the most reliable value of K_d for the unlabeled phosphoisoprenoid is obtained by keeping the K_d for the labeled ligand constant during the fitting procedure.

Data analysis was performed via a least-squares fitting using the program SCIENTIST, where the following binding equilibria were implemented (see the Supporting Information for the input script).

$$E + \text{mant-S} \rightleftarrows E-\text{mant-S} \qquad K_{d-mant}$$

$$E + \text{unlabeled S} \rightleftarrows E-\text{unlabeled S} \qquad K_{d-unlabeled}$$

During the least-squares fitting, K_{d-mant}, which was determined in an independent experiment, was held constant and $K_{d-unlabeled}$ was allowed to vary.

Global Fitting Procedures for Stopped-Flow Experiments. Data collection for the global fit procedures was carried out in two stages. First, stopped-flow traces were collected using different concentrations of *N*-methylanthraniloyl-labeled phosphoisoprenoid mixed with constant concentrations of GGTase-II. Global fitting of the experiments (typically four

traces) was used to determine the rate constants and fluorescence yields for the binding of the fluorescent isoprenoid to GGTase-II. The parameters were determined using a numerical integration procedure of a set of differential equations describing the binding model. The program that was used was SCIENTIST (MicroMath Scientific Software), and the following differential equations (system 1) were used to describe the model (for the SCIENTIST input script, see the Supporting Information).

$$E + A \underset{k_{-1}}{\overset{k_{+1}}{\rightleftharpoons}} EA_1 \underset{k_{-2}}{\overset{k_{+2}}{\rightleftharpoons}} EA_2$$

$$dE/dt = [EA_1]k_{-1} - [A][E]k_{+1}$$

$$dA/dt = [EA_1]k_{-1} - [A][E]k_{+1}$$

$$d[EA_1]/dt = [E][A]k_{+1} + k_{-2}[EA_2] - [EA_1](k_{+2} + k_{-1})$$

$$d[EA_2]/dt = [EA_1]k_{+2} - k_{-2}[EA_2]$$

The fluorescence (F) was defined as F = yield1[A_1] + yield2[EA_1] + yield3[EA_2] + offset.

To obtain the data for unlabeled isoprenoids, a mixture of mant-labeled phosphoisoprenoid and varying concentrations of unlabeled isoprenoid were mixed with a constant concentration of GGTase-II. All instrument settings, in particular, the photomultiplier voltage, were kept constant. The previously determined fluorescent yields and rate constants for the fluorescently labeled phosphoisoprenoid were used in the analysis of the competitive experiments. Knowing the binding parameters and fluorescent yields of the fluorescently labeled substrate, we were able to extract the binding parameters of the nonlabeled substrate. The fluorescent changes could be inferred from the first stage to the second, since the photomultiplier voltage remained constant. The following differential equations (system 2), describing the binding of the unlabeled substrate, for example, GGpp or Fpp, were used in the analysis:

$$E + B \underset{k_{-3}}{\overset{k_{+3}}{\rightleftharpoons}} EB_1 \underset{k_{-4}}{\overset{k_{+4}}{\rightleftharpoons}} EB_2$$

$$dE/dt = [EB_3]k_{-3} - [B][E]k_{+3}$$

$$dB/dt = [EB_1]k_{-3} - [B][E]k_{+3}$$

$$d[EB_1]/dt = [E][B]k_{+3} + k_{-4}[EB_2] - [EB_1](k_{+4} + k_{-3})$$

$$d[EB_2]/dt = [EB_1]k_{+4} - k_{-4}[EB_2]$$

Since GGpp and Fpp do not fluoresce, they do not contribute to the signal. The fluorescence (F) is therefore only determined by mant-labeled compounds described by eq 1:

$$F = \text{offset} + \text{yield1}[EA_1] + \text{yield2}[EA_2] \qquad (1)$$

RESULTS

Development of a Fluorescence Assay for the GGTase-II Interaction with Phosphoisoprenoids. The focus of this study was to investigate the lipid substrate specificity of GGTase-II. This requires an in vitro assay system which allows the determination of affinities and binding kinetics of different phosphoisoprenoid substrates. Initial attempts to use changes in the intrinsic tryptophan fluorescence of GGTase-II as a signal for these measurements were unsuccessful due to small intensity changes. In a different approach, we employed two fluorescent *N*-methylanthraniloyl-labeled isoprenoid derivatives that were demonstrated to act as substrates of GGTase-II in vitro (*14*) and will be subsequently termed mGpp and mFpp (Scheme 1). The chain lengths of mGpp and mFpp are comparable to those of farnesyl and geranylgeranyl pyrophosphate, respectively. Excitation scans of mFpp revealed that the fluorescence spectrum had an excitation maximum at 340 nm. The emission maximum was determined to be 435 nm (Figure 1). Addition of excess of GGTase-II to a solution of mFpp resulted in an approximately 90% increase in fluorescence with a blue shift in the emission spectrum (maximum of 426 nm). A 300% fluorescence increase was observed if mFpp was excited at 289 nm using fluorescence energy transfer (FRET) from tryptophans to the mant group (data not shown). The spectroscopic properties of mGpp were very similar to those of mFpp (data not shown).

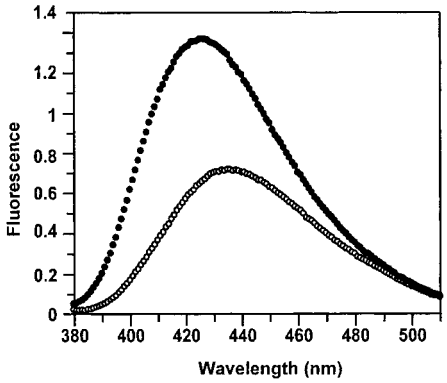

FIGURE 1: Emission scans of mFpp in the absence (○) and presence (●) of GGTase-II. The excitation wavelength was 340 nm, and 150 nM mFpp was used in both experiments. The concentration of GGTase-II was 500 nM.

Scheme 1: Phosphoisoprenoids Used in This Investigation

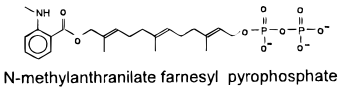
N-methylanthranilate farnesyl pyrophosphate

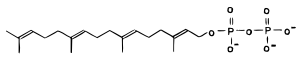
Geranylgeranyl pyrophosphate

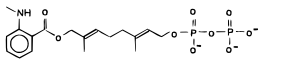
N-methylanthranilate geranyl pyrophosphate

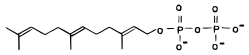
Farnesyl pyrophosphate

Affinity of GGTase-II for mFpp and GGpp. Determination of the affinity of GGTase-II for GGpp was performed in two stages. First, the affinity of GGTase-II for mFpp was determined via direct titration of GGTase-II versus mFpp. Then, a competitive titration of GGTase-II against a mixture of mFpp and GGpp was carried out to allow calculation of the affinity of GGTase-II for GGpp.

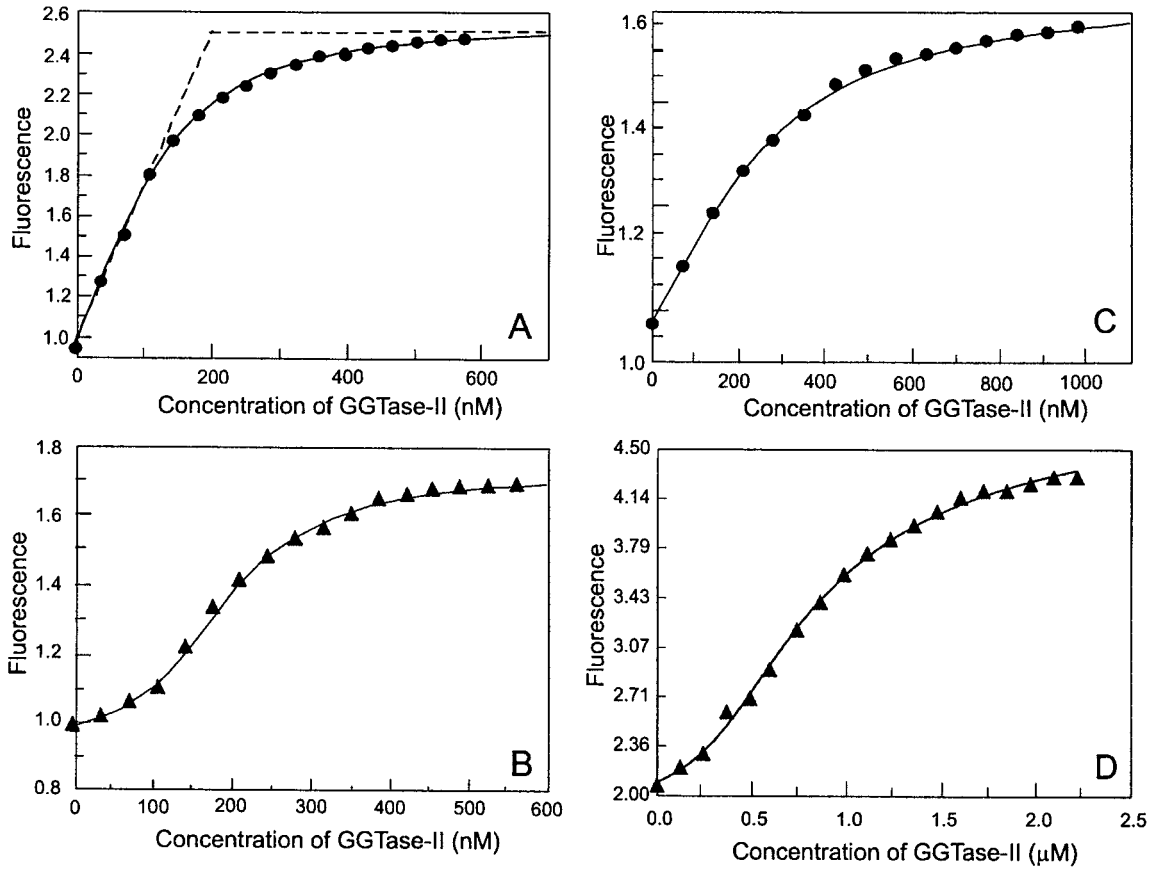

FIGURE 2: (A) Fluorescence titration of mFpp (200 nM) vs increasing concentrations of GGTase-II. The experimental curve was fitted resulting in a K_d of 49 ± 5 nM. It can be inferred from the intersection of the straight lines that 1 mol of GGTase-II was bound to 1 mol of mFpp. (B) Competitive titration where 150 nM mFpp was mixed with 150 nM GGpp. The mixture was titrated with increasing concentrations of GGTase-II. The K_d determined form the fit for GGpp was 8 ± 4 nM. (C) Fluorescence titration of mGpp (400 nM) vs increasing concentrations of GGTase-II. The experimental curve was fitted, resulting in a K_d of 330 ± 40 nM. (D) Competitive titration where 100 nM mGpp was mixed with 160 nM Fpp. The mixture was titrated against increasing concentrations of GGTase-II. The K_d determined form the fit for Fpp was 60 ± 8 nM.

The titration of 200 nM mFpp with increasing concentrations of GGTase-II is shown in Figure 2A. The experimental data were fitted using a quadratic equation yielding a K_d of 49 ± 5 nM (Figure 2A). It can also be inferred from the fit that one isoprenoid molecule is bound per molecule of GGTase-II, in agreement with what has previously been reported (*12*). The affinity of GGTase-II for mFpp was not significantly different when the experiment was performed in the presence of 10 mM EDTA, indicating that the presence of Mg^{2+} or other divalent metal ions was not required for phosphoisoprenoid binding (data not shown).

The titration was subsequently carried out under competitive conditions to determine the K_d for the interaction of GGTase-II with its natural substrate GGpp. In this experiment, 150 nM mFpp was mixed with 150 nM GGpp and the resulting solution was titrated with increasing concentrations of GGTase-II. As can be seen in Figure 2B, there is an initial lag in the fluorescence increase (see Materials and Methods). This is explained by GGpp binding more strongly than mFpp to the transferase, initially resulting in the formation of a fluorescently silent complex. However, at higher GGTase-II concentrations, the enzyme forms a complex with mFpp, causing an increase in fluorescence intensity. The data were fitted numerically using the program SCIENTIST and led to a K_d value of 8 ± 4 nM for the GGpp−GGTase-II interaction (Figure 2B).

Affinity of GGTase-II for mGpp and Fpp. A similar strategy was employed to determine the affinity of the GGTase-II for Fpp. The affinity of the enzyme for mGpp was determined, resulting in a K_d value of 330 ± 40 nM (Figure 2C). In a competitive experiment, 100 nM mGpp was combined with 460 nM Fpp and the mixture was subsequently titrated with increasing concentrations of GGTase-II. The curves obtained under these conditions are also sigmoidal, indicating that GGTase-II binds more tightly to Fpp than to mGpp. The affinity for Fpp was determined to be 60 ± 8 nM (Figure 2D).

Transient Kinetics of mFpp and GGpp Interaction with GGTase-II. Having obtained the steady-state parameters of phosphoisoprenoid binding, we proceeded to characterize the kinetic rate constants for this process. The signal from fluorescence resonance energy transfer from tryptophan to the mant group of the phosphoisoprenoid, i.e., exciting at 289 nm and measuring the fluorescence emission at 435 nm, proved to be very suitable for transient kinetic measurements.

Stopped-flow experiments were carried out at 25 °C using 50 nM GGTase-II in the presence of increasing concentrations of mFpp. Typical stopped-flow traces are shown in Figure 3a. Primary data analysis indicated that stopped-flow transients are not single-exponential functions, even when experiments were performed under pseudo-first-order conditions. This indicates that mFpp binding to GGTase-II is a

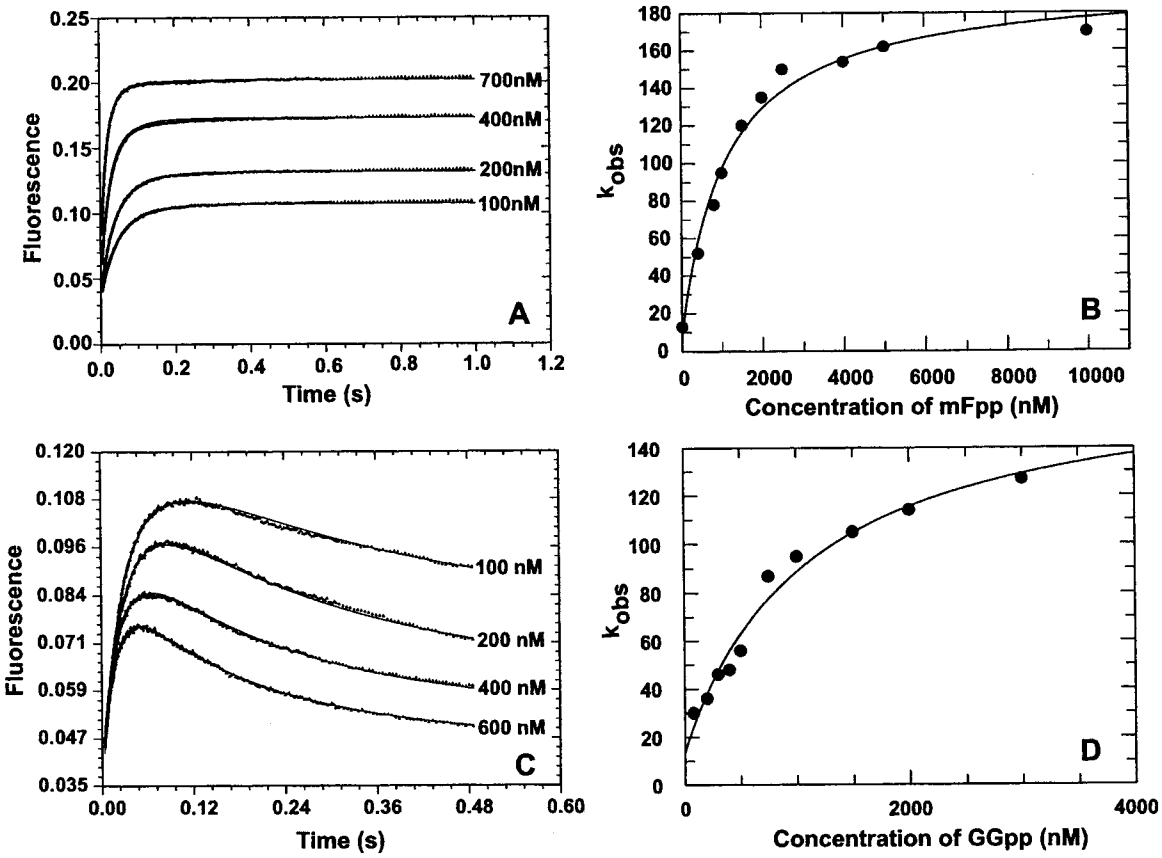

FIGURE 3: Stopped-flow traces of GGTase-II rapidly mixed with mFpp (A) or a mixture of mFpp and GGpp (C). The signal was based on fluorescence resonance energy transfer, exciting at 289 nm, while data collection was performed with a 398 nm cutoff filter. In panel A, 50 nM GGTase-II was mixed with increasing concentrations of mFpp (100, 200, 400, and 700 nM). The obtained fit resulted in the following rate constants: $k_{on} = 0.08\ s^{-1}\ nM^{-1}$, $k_{-1} = 16\ s^{-1}$, $k_{+2} = 6.7\ s^{-1}$, and $k_{-2} = 16\ s^{-1}$. Panel B shows the observed rate constant for the fast phase obtained by fitting the traces such as the ones shown in panel A to a sum of two exponentials. The K_s determined from this plot is 1100 nM; $k_{+1} = 187.7\ s^{-1}$, and $k_{off} = 8.4\ s^{-1}$. In panel C, 100 nM GGTase-II was mixed with 100 nM mFpp and increasing concentrations of GGpp (100, 200, 400, and 600 nM). The fit indicates that $k_{on} = 0.064\ s^{-1}\ nM^{-1}$, $k_{-1} = 1.9\ s^{-1}$, $k_{+2} = 1.0\ s^{-1}$, and $k_{-2} = 0.3\ s^{-1}$. Panel D shows the observed rate constant for the fast phase obtained by fitting the traces such as the ones shown in panel A to a sum of two exponentials. The K_s determined from this plot is 1099 nM; $k_{+1} = 157.98\ s^{-1}$, and $k_{off} = 13.6\ s^{-1}$.

multistep process. Data analysis was carried out assuming that mFpp binds in two steps to GGTase-II. The data were fitted using numerical integration of a set of differential equations describing a two-step binding mechanism (see Materials and Methods). This procedure resulted in an excellent fit to the observed data (Figure 3A). On the basis of these fits, fluorescent yields for each species in combination with the following rate constants were determined: $k_{on} = 0.08\ s^{-1}\ nM^{-1}$, $k_{-1} = 16\ s^{-1}$, $k_{+2} = 6.7\ s^{-1}$, and $k_{-2} = 16\ s^{-1}$ (Scheme 2). The calculated K_d for mFpp based on these four rate constants is 140 nM, which is in reasonable agreement with the previously determined K_d of 49 ± 5 nM. To obtain an independent estimate of k_{+1} and k_{-1}, we fitted the observed data to a double-exponential function. Although fits of experimental data to the sum of two exponential functions do not have a direct physical meaning (*17*), this type of experiment can still be used to derive approximate rate constants for association and dissociation. This approach ignores the second phase of the transients, which is taken into account by the global fitting; however, it does not require numerical integration, and thereby independently helps to validate the global fits. The plots of the fast phase (k_{obs1}) versus the concentration of mFpp are shown in Figure 3B. It was evident from the plot that k_{obs1} saturates at high concentrations of mFpp. This is indicative of a two-step

Scheme 2: Nomenclature of Kinetic Rate Constants Used in This Study[a]

Two-step binding:

$$\text{RabGGTase + Xpp} \underset{k_{-1}}{\overset{k_{on}}{\rightleftharpoons}} \text{RabGGTase-Xpp}^{*} \underset{k_{-2}}{\overset{k_{+2}}{\rightleftharpoons}} \text{RabGGTase-Xpp}^{**}$$

Three-step binding:

$$\text{RabGGTase Xpp} \overset{K_S}{\rightleftharpoons} \text{RabGGTase-Substrate} \underset{k_{-1}}{\overset{k_{+1}}{\rightleftharpoons}} \text{RabGGTase-Xpp}^{*} \underset{k_{-2}}{\overset{k_{+2}}{\rightleftharpoons}} \text{RabGGTase-Xpp}^{**}$$

[a] Xpp represents the phosphoisoprenoid substrate.

binding mechanism, with the first step comprising a rapid equilibrium followed by a slow second step. The curve was fitted to the appropriate equation $k_{obs} = 1/(1 + K_s/[mFpp])\text{-}k_{+1} + k_{-1}$ (*18*). K_s was found to be 1100 nM. k_{+1} was 187 s^{-1}, while k_{off} was estimated to be 8.4 s^{-1}. The dissociation rate constant k_{-1} was determined by displacement in an independent experiment to be 12 s^{-1} (data not shown).

Observation of saturable behavior for the fast rate of a biphasic transient (k_{obs1} in Figure 3B) indicates that the reaction consists of at least three steps: a fast initial

equilibrium with an equilibrium constant K_s of 1100 nM with no change in the fluorescence signal, followed by two further steps, both of which give rise to a change in the fluorescent signal. The data used for the global fit analysis were recorded at concentrations significantly smaller than the K_s (Figure 3A,B). The second-order rate constant (k_{on}) therefore relates to the first-order rate constant k_{+1} by the equation $k_{+1} = k_{on}K_s = 0.08\ nM^{-1}\ s^{-1} \times 1100\ nM = 88\ s^{-1}$ (Scheme 2) (*19*). After this conversion, a k_{+1} of 88 s^{-1} is in reasonable agreement with the independently determined k_{+1} of 187 s^{-1}.

Having obtained data on the kinetics of GGTase-II interaction with mFpp, we sought to determine the kinetic parameters of GGpp binding. In this experiment, 100 nM GGTase-II was mixed with 100 nM mFpp and increasing concentrations of GGpp. An example of the fluorescent traces that were obtained is shown in Figure 3C. The shape of the stopped-flow transient obtained in Figure 3C can be rationalized in the following way. When mFpp binds, the fluorescence increases in the first part of the transient. Some GGpp is bound at the same time, but does not give rise to a fluorescence signal increase. The height of the inflection point and the rate of approach to it are dependent on the amount of GGpp present; the more GGpp is present with respect to mFpp, the larger the fraction of the enzyme occupied by GGpp, and therefore the lower the fluorescence of the inflection point. The observed rate, on the other hand, represents the approach to a pre-steady-state equilibrium and therefore equals the sum of the effective rate constants for mFpp and GGpp binding (*18*). A higher concentration of GGpp will result in a larger second-order rate constant for binding and will therefore lead to an increased rate of approach to the inflection point of the pre-steady-state equilibrium. Therefore, plotting the observed rate of approach to the pre-steady-state plateau provides information about the absolute association rates for GGpp. The decrease in the fluorescence in the second part of the transient is dependent on the relative dissociation rates of GGpp and mFpp. If the dissociation rate of mFpp is faster than that of GGpp, then, having approached the pre-equilibrium, mFpp will dissociate from GGTase-II and will be partially substituted by GGpp. At high concentrations of GGpp, all mFpp dissociates from the enzyme and is replaced with GGpp, and therefore, the rate of the fluorescent decrease under these conditions should represent the genuine k_{off} rate for mFpp. It should be noted that transients of this type can only occur if the effective association rates (k_{on} multiplied by the concentration of the substrate) of mFpp and GGpp are comparable, while the dissociation rate of the labeled compound is faster than that of the unlabeled one.

The exact relationships between the binding and dissociation rates of GGpp in this experiment are complex and can only be determined using numerical fitting. The fitting procedure described in Materials and Methods was used to determine the following rate constants for GGpp: $k_{on} = 0.064\ s^{-1}\ nM^{-1}$, $k_{-1} = 1.9\ s^{-1}$, $k_{+2} = 1.0\ s^{-1}$, and $k_{-2} = 0.3\ s^{-1}$. To be able to carry out the global fits, the fluorescent yields and rate constant obtained for mFpp (Figure 3A) were used in the analysis. Best fits were obtained when the binding of GGpp was modeled as consisting of at least two steps.

To validate some aspects of the data via techniques other than global fitting, stopped-flow traces were analyzed using double-exponential functions. As indicated above, plotting the obtained rate constant for the increase in fluorescence against the concentration of GGpp provides information about the association rates for GGpp. As can be seen in Figure 3D, the observed association rate of GGpp reaches saturation at high concentrations of GGpp. The first phase increases to a maximal value of 140 s^{-1} with a half-maximal value at 1099 nM, and $k_{+1} = 80\ s^{-1}$. In analogy to what has been said for mFpp, we conclude that a rapid pre-equilibrium exists which does not involve a signal change. Since the global fits were carried out at low substrate concentrations with respect to K_s, we can convert the second-order binding constant of the global fit, k_{on} (Figure 3D), into a first-order rate constant via the relationship $k_{+1} = k_{on}K_s = 0.064\ nM^{-1}\ s^{-1} \times 1099\ nM = 70\ s^{-1}$. This is in excellent agreement with the independently determined k_{+1} of 80 s^{-1}. In addition, the calculated K_d based on the rate constants determined by the global fit is 7 nM, which matches closely the experimentally determined K_d of 8 ± 4 nM.

Transient Kinetics of mGpp and Fpp Binding. We applied an identical strategy in the analysis of mGpp and Fpp binding to GGTase-II. The transients of association of GGTase-II with mGpp also followed double-exponential behavior. Numerical fitting was carried out, and the following rate constants were obtained (Figure 4A): $k_{+1} = 0.1\ s^{-1}\ nM^{-1}$, $k_{-1} = 62\ s^{-1}$, $k_{+2} = 117\ s^{-1}$, and $k_{-2} = 89.1\ s^{-1}$. Best fits to the experimental data were achieved assuming a two-step binding mechanism. The calculated K_d based on these rate constants was 267 nM, in good agreement with the experimentally determined K_d of 330 ± 12 nM. There was, however, no sign of saturation of the association rates even at the highest concentrations that were tested (4 μM) (Figure 4B). This could be due to either the absence of a rapid pre-equilibrium or a pre-equilibrium with a much higher K_s. The association rate (k_{+1}) was determined independently from a linear fit of Figure 4B to be 0.09 $nM^{-1}\ s^{-1}$, and k_{-1} was determined in an independent displacement experiment to be 63 s^{-1} (data not shown). Both values fit well with the rate constants obtained from the global fit.

To determine the rate of Fpp binding to GGTase-II, we rapidly mixed 50 nM GGTase-II with 50 nM mGpp and increasing concentrations of Fpp. The result of a typical experiment is shown in Figure 4C. As in the case of mFpp, mGpp could compete with Fpp in the initial binding but was displaced by it in the following step. We used numerical fitting to determine the rate constants for Fpp: $k_{+1} = 0.1\ s^{-1}\ nM^{-1}$ and $k_{-1} = 4.8\ s^{-1}$. Fits of sufficient quality were obtained assuming single-step binding. The data were also fitted as a sum of two exponential functions and were plotted against substrate concentration (Figure 4D). We could not observe saturation of the rate of the first phase even at the highest concentrations of Fpp that were tested. This also indicates that Fpp has no or a very low affinity pre-equilibrium. The calculated K_d based on the above-mentioned rate constants for Fpp is 47 nM and is in good agreement with the K_d measured in direct titration (60 ± 8 nM).

Affinity of the Ternary Complex for GGpp and Fpp. As pointed out in the introductory section, GGTase-II performs its function in concert with another protein termed REP. We demonstrated recently that Rab, REP, and GGTase-II form a tight ternary complex (*15*). It is therefore possible that the affinity for the lipid substrate is influenced by complex formation. To determine the affinity of different isoprenoids for the GGTase-II−REP-1−Rab7 complex, we used a mutant

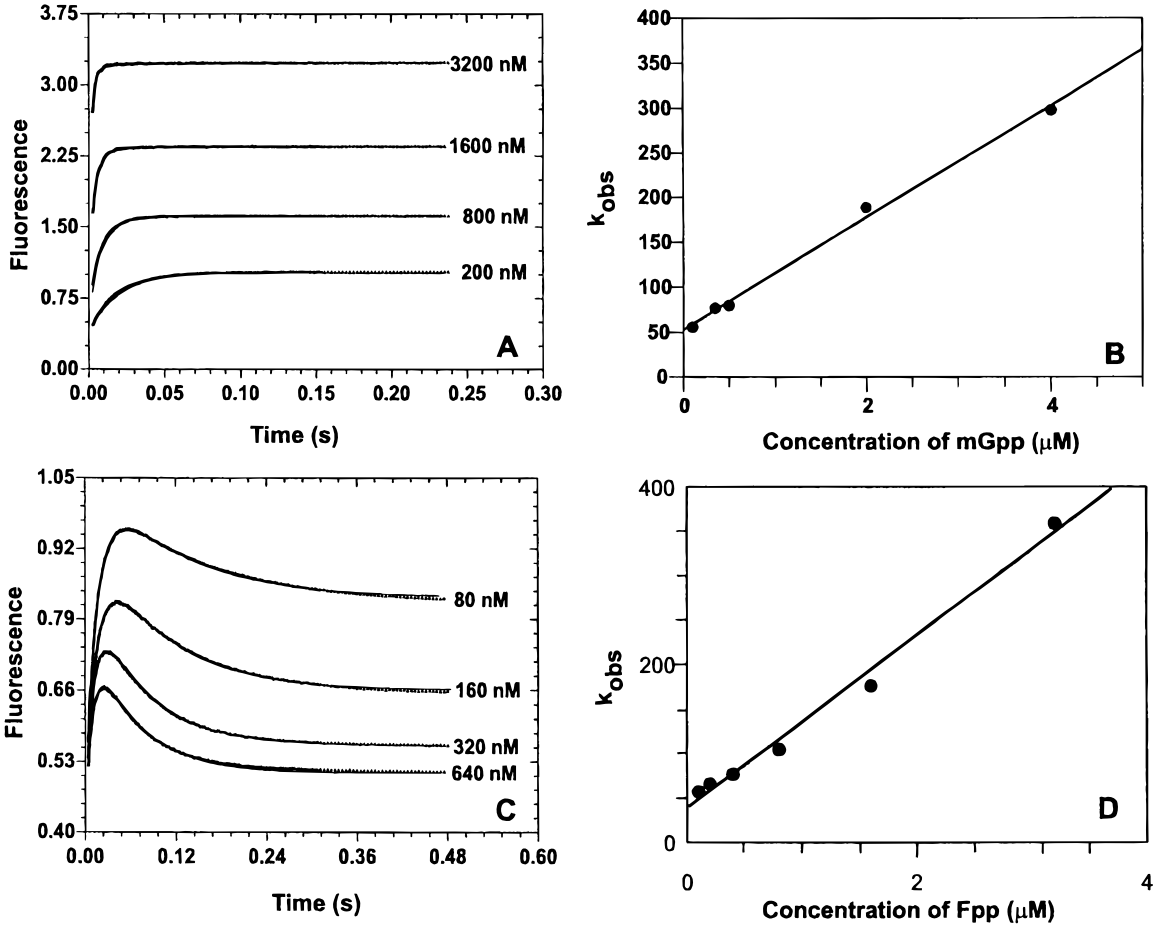

FIGURE 4: Stopped-flow traces of GGTase-II rapidly mixed mGpp (A) or a mixture of mGpp and Fpp (C). The signal was based on fluorescence resonance energy transfer, exciting at 289 nm, measuring the fluorescence with a 398 nm cutoff filter. In panel A, 50 nM GGTase-II was mixed with increasing concentrations of mGpp (200, 800, 1600, and 3200 nM). The obtained fit resulted in the following rate constants: $k_{on} = 0.1\ s^{-1}\ nM^{-1}$, $k_{-1} = 62\ s^{-1}$, $k_{+2} = 117\ s^{-1}$, and $k_{-2} = 89.1\ s^{-1}$. Panel B shows the observed rate constant for the fast phase obtained by fitting the traces such as the ones shown in panel A to a single-exponential function. In panel C, 150 nM GGTase-II was mixed with 100 nM mFpp and increasing concentrations of GGpp (80, 160, 320, and 640 nM). Panel D shows the observed rate constant for the fast phase obtained by fitting the traces such as the ones shown in panel A to a sum of two exponentials.

Rab7-SS, where two C-terminal cysteines, C205 and C207, are replaced with serine residues. This mutant does not undergo prenylation and thus allows reversible equilibrium titrations to be carried out. Previous studies (*15*) established that GGTase-II binds the Rab7−Rep1 complex with a K_d very similar to that of the Rab7-SS−REP-1 complex, showing that the double-cysteine mutation of Rab7 has very little effect on the affinities. We used the purified ternary complex to ensure that stoichiometric amounts of REP-1, Rab7-SS, and GGTase-II were present during these measurements. The reversible equilibrium titration with the fluorescent analogue mFpp was performed essentially as described for GGTase-II alone.

The binding of the ternary complex to mFpp was characterized in the first step. To this end, 300 nM mFpp was titrated with increasing concentrations of mFpp. Examination of the titration curve revealed that only 60% of the purified ternary complex was active in phosphoisoprenoid binding due to a currently unknown reason (data not shown). However, we suspect that inactivation is at least partially due to oxidation or aggregation of this complex which combines 36 cysteine residues, even in the presence of reducing agents. If it was assumed that 40% of the ternary complex is inactive, a K_d value of 183 nM was obtained. To determine the affinities of GGpp and Fpp for the ternary complex, a cotitration strategy was employed, yielding K_ds of 13 ± 8 and 260 ± 30 nM, respectively (Figure 5B). The latter result indicates that the affinity GGTase-II for Fpp is significantly affected upon ternary complex formation.

In Vitro Prenylation Using GGpp and Fpp as Substrates. The binding data described above indicate that GGTase-II can bind both Fpp and GGpp. Moreover, we have previously demonstrated that both mGpp and mFpp could be transferred onto Rab7 by GGTase-II (*14*), suggesting that Fpp could also act as a prenyl donor. A well-established in vitro prenylation assay (*16*) with Rab7 as a protein substrate was used to investigate this further. In a typical setup, the Rab7−REP-1 complex at a final concentration of 1 μM was mixed with 1 μM GGTase-II and an excess of tritium-labeled substrate at the beginning of reaction. Prenylation of Rab7 was followed over time in the presence of 3 μM [^{3}H]farnesyl pyrophosphate (Figure 6A). The experiment indicated that farnesyl pyrophosphate acted as an isoprenoid donor to Rab7 with an observed rate constant of 0.082 ± 0.05 s^{-1}. When the same experiment was carried out in the presence of 3 μM [^{3}H]geranylgeranyl pyrophosphate, an almost identical prenylation rate of 0.092 ± 0.05 s^{-1} was observed (Figure 6B). The reaction corresponds to a first-order process and was fitted to a single-exponential function to obtain the observed rate constant. The observed rate in this concentra-

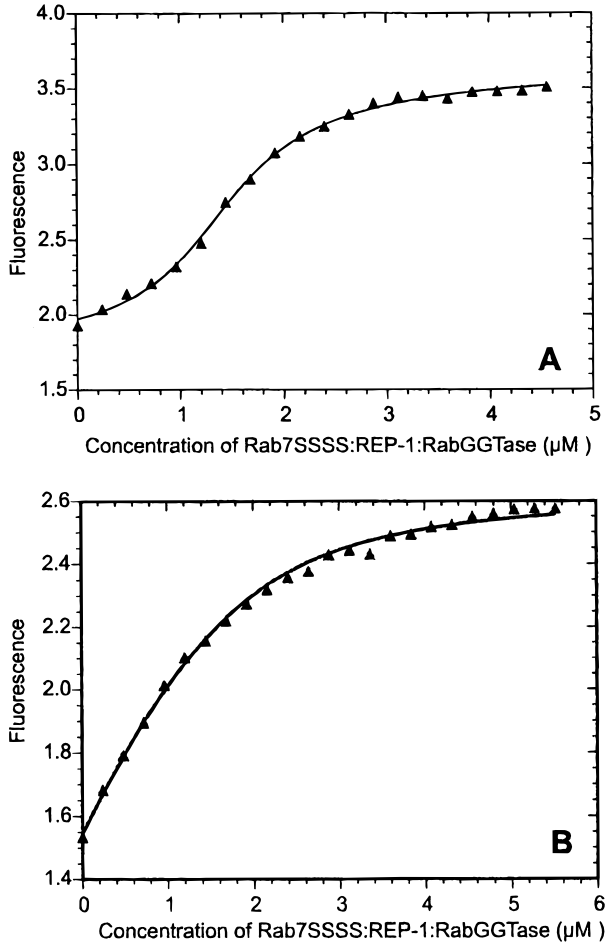

FIGURE 5: (A) Competitive fluorescence titration of mFpp (600 nM) mixed with 600 nM GGpp vs increasing concentrations of the GGTase-II−Rep1−Rab7-SS complex. The K_d was determined to be 13 ± 8 nM. (B) Like panel A but using 600 nM Fpp and 600 nM mFpp. The fit resulted in a K_d for Fpp binding to the GGTase-II−REP-1−Rab7-SS complex of 260 ± 30 nM.

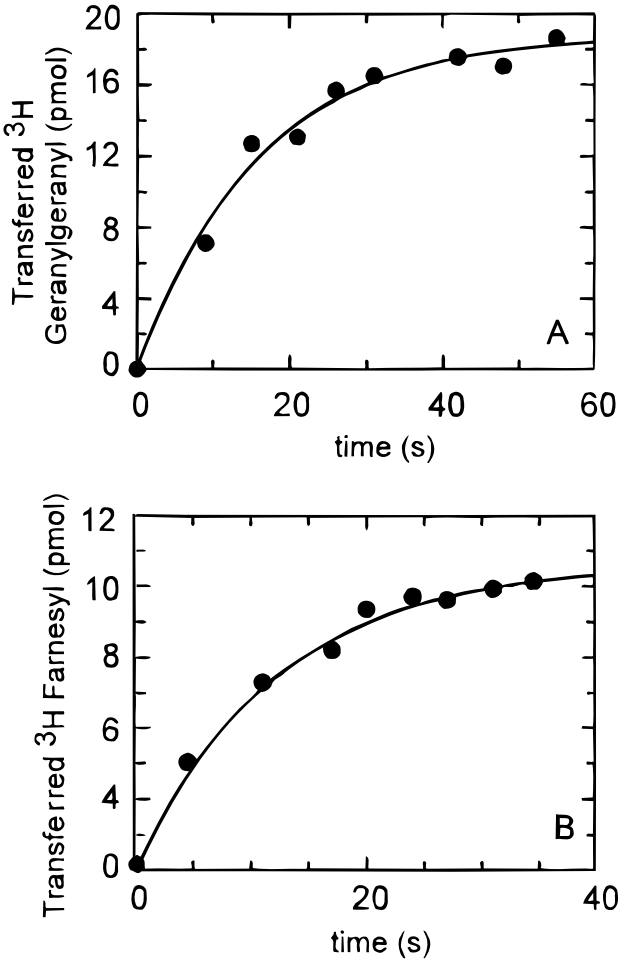

FIGURE 6: In vitro prenylation assay using ^{3}H-labeled substrates. (A) Extent of incorporation of [^{3}H]geranylgeranyl in Rab7 catalyzed by GGTase-II. The solid line represents a single-exponential fit with a k_{obs} of 0.06 ± 0.007 s^{-1}. (B) Amount of [^{3}H]farnesyl transferred onto Rab7. The solid line represents a single-exponential fit with a k_{obs} of 0.081 ± 0.01 s^{-1}.

tion regime corresponds to the rate of the actual prenylation chemistry, and does not have any contribution from substrate binding or product release. Interestingly, the two isoprenoids differed somewhat in their respective transfer efficiencies. However, this does not have any effect on the determination of the rate. The difference in observed amplitude was not due to differences in binding affinities since the use of higher concentrations of Fpp did not result in increased amounts of prenylated Rab7 (data not shown). To ascertain that Fpp was not converted into GGpp in the course of the prenylation reaction, we incubated purified GGTase-II and REP-1 in the presence of [^{3}H]Fpp. Analysis of the reaction mixture by thin-layer chromatography demonstrated that Fpp was not converted to any higher-order phosphoisoprenoids (data not shown).

In summary, the prenylation experiments clearly indicate that Fpp is a substrate for GGTase-II and that its rate of transfer, under saturating conditions, is similar to that of GGpp.

DISCUSSION

Development of a Fluorescence Assay for the GGTase-II−Phosphoisoprenoid Interaction. We have developed a highly sensitive fluorescence assay to monitor interactions of GGTase-II with its lipid substrates. The assay takes advantage of large changes in fluorescence intensity upon mFpp and mGpp binding to GGTase-II. Especially large changes are observed when the fluorescence of the *N*-methylanthraniloyl group is excited by energy transfer from tryptophan residues. This is consistent with the presence of tryptophan in the active site of GGTase-II as indicated by the high-resolution structure of GGTase-II (*6*).

Longer Isoprenoid Substrates Are Bound More Tightly. Using this assay, we determined the K_ds of GGTase-II for GGpp and Fpp to be 60 ± 8 and 8 ± 4 nM, respectively. The affinity for mGpp was determined to be 330 ± 12 nM, while the K_d for mFpp was 49 ± 5 nM. It transpired from our data that the length of the isoprenoid correlates with affinity (Table 1). Geranylgeranyl pyrophosphate, the natural substrate and the longest phosphoisoprenoid that was used, is bound most tightly (K_d = 8 ± 4 nM), followed by the shorter mFpp (K_d = 49 ± 5 nM), which binds slightly tighter than Fpp (K_d = 60 ± 8 nM). Further shortening of the isoprenoid chain, as seen in case of mGpp, leads to a drastic decrease in affinity (K_d = 330 ± 12 nM).

Applying stopped-flow methodology, we were able to analyze the binding kinetics of these interactions. The rate constants derived for different isoprenoids demonstrate that

Table 1

	GGpp	mFpp	Fpp	mGpp
k_{-1} (s^{-1})	1.9	16	4.8	62
k_{on} (s^{-1} nM^{-1})	0.064	0.063	0.11	0.10
k_{+2} (s^{-1})	1	6.7	−	117.5
k_{-2} (s^{-1})	0.3	16	−	89.1
K_s (nM)	1200	1400	−	−
K_d (nM)	9 ± 4	49 ± 5	60 ± 8	330 ± 12
K_{dcalc}[a] (nM)	7.7	140	44	267

[a] K_d calculated from the measured rate constants.

Table 2

	mFpp	GGpp	Fpp
K_d in the presence of RabGGTase (nM)	49 ± 5	8 ± 4	60 ± 8
K_d in the presence of the RabGGTase−REP-1−Rab7 complex (nM)	183	13 ± 8	260 ± 30

all the substrates tested have similar second-order association rate constants. The difference in affinities is largely due to variations in the dissociation rates (Table 1). The tightest binding substrate, GGpp ($K_d = 8 \pm 4$ nM), has a dissociation rate constant k_{-1} of 1.9 s^{-1}; mFpp ($K_d = 49 \pm 5$ nM) has a k_{-1} of 16 s^{-1}, while mGpp possesses the lowest affinity ($K_d = 330 \pm 12$ nM) with a k_{-1} of 62 s^{-1}.

The Binding Mechanism of Fpp Differs from That of GGpp. The mechanism distinguishing between Fpp and GGpp is, however, not based only on a difference in dissociation rates. Binding of GGpp to GGTase-II consists of at least three binding steps: an initial rapid pre-equilibrium followed by two isomerization events. The binding mechanism of Fpp on the other hand can be described adequately as a single-step binding. A rapid pre-equilibrium could not be detected in this case, probably due to its equilibrium constant being very small. A comparison of the binding parameters of Fpp and GGpp (Table 1) indicated that GGTase-II initially binds Fpp and GGpp with little discrimination. However, once GGpp is bound, a conformational change appears to occur that further tightens binding. When all the kinetic binding data are summed up, it seems that GGTase-II proofreads phosphoisoprenoid substrates at different levels (Table 1). While GGTase-II discriminates between mFpp and in particular mGpp on the basis of their dissociation rates, probably due to the bulky *N*-methylanthraniloyl group, Fpp and GGpp discrimination is mainly achieved in a subsequent step. The exact molecular nature of this latter proofreading step, which tightens binding for GGpp but not for Fpp, requires further investigation.

Comparison of GGTase-II with Other Prenyltransferases. The degree of discrimination between different isoprenoids as well as the kinetic mechanism established for GGTase-II shows similarities to FTase. Kinetic investigations on FTase established a two-step binding mechanism where a rapid initial step with an equilibrium constant of 10 μM is followed by a concentration-independent isomerization step (*20*). However, the FTase reaction proceeds with an association rate constant of 0.004 nM^{-1} s^{-1} combined with a dissociation rate k_{-1} of 0.012 s^{-1}. Thus, both forward and reverse reactions progress with rate constants that are much slower than that observed for GGTase-II. Determination of the affinities of FTase and GGTase-I toward their substrate indicated that both enzymes bind their respective lipid substrates tightly. Yokoyama et al. showed that GGTase-I binds GGpp with an affinity of 3 nM and Fpp with an affinity of 1 μM (*21*). FTase binds Fpp with an affinity of about 2.8 nM (*20*) and GGpp with a K_d of about 30 nM, thereby discriminating only between the two phosphoisoprenoids by a factor of 10. As shown here, GGTase-II also does not strongly discriminate between GGpp and Fpp, displaying a maximal factor of 20 in favor of GGpp.

The Affinity of the GGTase-II−REP-1−Rab7 for Isoprenoids Is Lower Than That of GGTase-II Alone. GGTase-II performs its function in concert with another protein termed REP. Prenylation can only occur when its protein substrate, Rab7 in this investigation, is in complex with REP protein. The affinities of GGpp and Fpp were therefore also analyzed when GGTase-II was in complex with REP-1 and Rab7. Using a mutant of Rab7 which had serines in place of the cysteine residues used for prenylation (Rab7-SS C205S/C207S), we determined the affinities of the complex for mFpp, GGpp, and Fpp. In the presence of the REP-1−Rab7 complex, the K_d values for GGpp, mFpp, and Fpp were lowered by 1.6-, 3.7-, and 4.3-fold, respectively, compared to that for GGTase-II alone. The affinity for GGpp binding to the ternary complex was 13 ± 8 nM, while Fpp was bound with an apparent affinity of 260 ± 30 nM. Overall, this represents a 7- and 20-fold difference in binding affinity of the natural substrate GGpp over Fpp for GGTase-II and the GGTase-II−REP-1−Rab7 complex, respectively. Since the equilibration of phosphoisoprenoid binding is much faster than the rate of prenylation, the K_d of the ternary complex should determine the selectivity of the enzyme in vivo.

Substrate Specificity of GGTase-II. Using [^{3}H]GGpp and [^{3}H]Fpp, we directly demonstrate that both isoprenoids could be transferred onto Rab7 by GGTase-II. This finding agrees with our earlier observation that GGTase-II can use both mGpp and mFpp as substrates (*14*). Seabra and co-workers (*12*) have previously performed competitive prenylation reactions with GGTase-II in the presence of the Rab7−REP-1 complex using an excess of substrate of 625 nM [^{3}H]-GGpp and increasing concentrations of unlabeled Fpp. The authors came to the conclusion that Fpp is not a substrate for GGTase-II under these conditions. However, it can be seen from their data (Figure 2 in ref *12*) that Fpp, at a concentration of 1600 nM, does decrease the prenylation amplitude by about 8−10%. This finding is consistent with the K_d values determined in this study for GGpp (13 ± 8 nM) and Fpp (260 ± 30 nM) in the presence of the Rabla−REP-1 complex; using a saturating GGpp concentration of 625 nM and almost saturating conditions of Fpp (1600 nM), one would expect that ≈15% {[K_d(GGpp)/[GGpp]]/[K_d(Fpp)/[Fpp]]} of the GGTase-II is bound to Fpp. This is in good agreement with the observation that Fpp, under the conditions that were used, could compete with GGpp for about 8−10% of the GGTase-II.

We believe that a 7−20-fold difference in affinity combined with high local concentrations of GGpp, or association of the enzyme with the geranylgeranylpyrophosphate synthase in vivo [as hypothesized by Deisenhofer and co-workers (*6*)], could easily account for the proposed specificity of the GGTase-II. Alternatively, there may be some degree of transfer of farnesyl groups onto Rab proteins. To our knowledge, there are no in vivo data that vigorously exclude such a possibility.

On the basis of the observed relatively small discrimination of GGTase-II between Fpp and GGpp, it seems likely that farnesyltransferase inhibitors could also, to some extent, inhibit GGTase-II. This finding has clinical relevance since farnesyltransferase inhibitors are promising substances in anticancer chemotherapy (*4*). If these drugs do indeed affect GGTase-II activity, the prenylation of Rab proteins in general would be impaired. It has recently been shown that a reduction in GGTase-II activity in mice bearing a *gunmetal* mutation leads to prolonged bleeding and thrombocytopenia (*22*). Thus, inhibition of GGTase-II may result in undesirable side effects in humans. This should be taken into consideration when characterizing inhibitors of farnesyltransferase intended for medical applications. The tools developed here allow these studies to be carried out with relative ease.

ACKNOWLEDGMENT

We are very grateful to Miguel C. Seabra for stimulating discussions. We are also indebted to Michelle O'Reilly and Alexandru-Tudor Constantinescu for critically reading the manuscript. Jerome Huppertz is acknowledged for help with the kinetics measurements and Stefan Uttich for invaluable technical assistance. N.H.T. was supported by the EMBO long-term fellowship.

SUPPORTING INFORMATION AVAILABLE

SCIENTIST input script for analysis of the competitive stopped-flow experiments assuming a two-step binding model and for analysis of the competitive titrations. This material is available free of charge via the Internet at http://pubs.acs.org.

REFERENCES

1. Glomset, J. A., and Farnsworth, C. C. (1994) *Annu. Rev. Cell Biol. 10*, 181−205.
2. Gelb, M. H. (1997) *Science 275*, 1750−1751.
3. Gelb, M. H., Scholten, J. D., and Sebolt-Leopold, J. S. (1998) *Curr. Opin. Chem. Biol. 2*, 40−48.
4. Rowinsky, E. K., Windle, J. J., and Von Hoff, D. D. (1999) *J. Clin. Oncol. 17*, 3631−3652.
5. Casey, P. J., and Seabra, M. C. (1996) *J. Biol. Chem. 271*, 5289−5292.
6. Zhang, H., Seabra, C. M., and Deisenhofer, J. (2000) Crystal structure of Rab geranylgeranyltransferase at 2.0 Å resolution. *Structure 8*, 241−251.
7. Long, S. B., Casey, P. J., and Beese, L. S. (2000) *Struct. Folding Des. 8*, 209−222.
8. Seabra, M. C., Goldstein, J. L., Sudhof, T. C., and Brown, M. S. (1992) *J. Biol. Chem. 267*, 14497−14503.
9. Seabra, M. C., Brown, M. S., Slaughter, C. A., Sudhof, T. C., and Goldstein, J. L. (1992) *Cell 70*, 1049−1057.
10. Alexandrov, K., Horiuchi, H., Steele-Mortimer, O., Seabra, M. C., and Zerial, M. (1994) *EMBO J. 13*, 5262−5273.
11. Wilson, A. L., Erdman, R. A., and Maltese, W. A. (1996) *J. Biol. Chem. 271*, 10932−10940.
12. Desnoyers, L., and Seabra, M. C. (1998) *Proc. Natl. Acad. Sci. U.S.A. 95*, 12266−12270.
13. Yokoyama, K., Trobridge, P., Buckner, F. S., Scholten, J., Stuart, K. D., Van Voorhis, W. C., and Gelb, M. H. (1998) *Mol. Biochem. Parasitol. 94*, 87−97.
14. Owen, D. J., Alexandrov, K., Rostkova, E., Scheidig, A. J., Goody, R. S., and Waldmann, H. (1999) *Angew. Chem., Int. Ed. 38*, 509−512.
15. Alexandrov, K., Simon, I., Yurchenko, V., Iakovenko, A., Rostkova, E., Scheidig, A. J., and Goody, R. S. (1999) *Eur. J. Biochem. 265*, 160−170.
16. Armstrong, S. A., Brown, M. S., Goldstein, J. L., and Seabra, M. C. (1995) *Methods Enzymol. 257*, 30−41.
17. Gutfreund, H. (1995) *Kinetics for the life sciences*, Chapter 6, Cambridge University Press, New York.
18. Hiromi, K. (1979) *Kinetics of fast enzyme reactions: theory and practice*, Chapter 1, Halsted Press, Tokyo.
19. Johnson, K. A. (1992) *Enzymes 20*, 1−61.
20. Furfine, E. S., Leban, J. J., Landavazo, A., Moomaw, J. F., and Casey, P. J. (1995) *Biochemistry 34*, 6857−6862.
21. Yokoyama, K., McGeady, P., and Gelb, M. H. (1995) *Biochemistry 34*, 1344−1354.
22. Detter, J. C., Zhang, Q., Mules, E. H., Novak, E. K., Mishra, V. S., Li, W., McMurtrie, E. B., Tchernev, V. T., Wallace, M. R., Seabra, M. C., Swank, R. T., and Kingsmore, S. F. (2000) *Proc. Natl. Acad. Sci. U.S.A. 97*, 4144−4149.

BI000835M